Açıkkalp, Emin; Chen, Lingen; Ahmadi, Mohammad Hossein

Article

Comparative performance analyses of molten carbonate fuel cell-alkali metal thermal to electric converter and molten carbonate fuel cell-thermo-electric generator hybrid systems

Energy Reports

Provided in Cooperation with:
Elsevier

Suggested Citation: Açıkkalp, Emin; Chen, Lingen; Ahmadi, Mohammad Hossein (2020) : Comparative performance analyses of molten carbonate fuel cell-alkali metal thermal to electric converter and molten carbonate fuel cell-thermo-electric generator hybrid systems, Energy Reports, ISSN 2352-4847, Elsevier, Amsterdam, Vol. 6, pp. 10-16, https://doi.org/10.1016/j.egyr.2019.11.108

This Version is available at:
https://hdl.handle.net/10419/244011

Energy Reports 6 (2020) 10–16

Contents lists available at ScienceDirect

Energy Reports

journal homepage: www.elsevier.com/locate/egyr

Research paper

Comparative performance analyses of molten carbonate fuel cell-alkali metal thermal to electric converter and molten carbonate fuel cell-thermo-electric generator hybrid systems

Emin Açıkkalp [a,b], Lingen Chen [c,*], Mohammad Hosein Ahmadi [d]

[a] Department of Mechanical Engineering, Engineering Faculty, Bilecik S.E. University, Bilecik, Turkey
[b] Energy Technology Application and Research Center, Bilecik S.E. University, Bilecik, Turkey
[c] Institute of Thermal Science and Power Engineering, Wuhan Institute of Technology, Wuhan 430205, China
[d] Faculty of Mechanical Engineering, Shahrood University of Technology, Shahrood, Iran

ARTICLE INFO

Article history:
Received 27 August 2019
Received in revised form 13 November 2019
Accepted 22 November 2019
Available online xxxx

Keywords:
Alkali metal electric converter
Thermoelectric generator
Molten carbonate fuel cell
Hybrid system
Performance

ABSTRACT

Purpose of this paper is to compare the performance of an alkali metal thermal electric converter (AMTEC) and thermoelectric generator (TEG) as a subsystem for utilizing rejected heat from the molten carbonate fuel cell (MCFC). AMTEC and TEG have various advantages such as; higher power density, no maintenance needed, silent and generally lower cost. Therefore, they have good potential to utilize waste heat. Performance parameters of systems are defined as power output density, exergy destruction rate density, energy and exergy efficiencies. Results show that the system MCFC-AMTEC hybrid system is more advantageous than the MCFC-TEG hybrid system. Some important results are listed follows; maximum power output densities for the MCFC-AMTEC and MCFC-TEG are 2425.833 (W/m^2), and 1964.389 (W/m^2), respectively, while efficiencies are %, 76.6% and 76.4 %.

1. Introduction

Nowadays, new technologies and applications are required to compensate for the energy need of the world, which has been increasing because of population growth and industrial development. In addition, these technologies must be efficient and environmental friendly. Thus, cogeneration systems, hybrid usage of renewable energies, and multigenerational application have been growing attention to utilize energy sources more efficient and more environmentally friendly. Alkali metal thermal electric converter (AMTEC) and thermoelectric generator (TEG) tools can be important alternatives.

The fuel cell is very popular because of their high efficiencies and the possibility of using great variation of fuel. Especially, high-temperature fuel cells like molten carbonate fuel cell (MCFC) present a great opportunity of utilizing combined systems. Therefore, MCFC based hybrid systems have been analyzed for different applications including hybrid systems. Hybrid systems based MCFC involving different type subsystems have been investigated in recent years, see Açıkkalp (2017a,b,c) and Ahmadi et al. (2018a,b).

Alkali metal thermal to the electric converter (AMTEC) may be an alternative subsystem for the MCFC as a hybrid system. AMTEC system is a very convenient application because of having high power density, no maintenance, no moving part, silent, using different sources and lower costs. Owing to these, AMTEC is good candidate to be utilized for military, domestic and aerospace applications. The disadvantage of the AMTEC is that heat is rejected on high temperatures and sometimes big portion of the heat is wasted. However, the high power density of AMTEC compensates this disadvantage. Weber (1974) proposed the AMTEC system firstly. Xiao et al. (2017) conducted a parametric analysis of condensation heat transfer characteristics of an AMTEC. Lee et al. (2017) investigated the effect of thermal radiation on the AMTEC experimentally and carried out simulations. Optimum operation conditions of the AMTEC were carried out by Peng et al. (2018). The analyzed parameters included electrode thickness, voltage output, current density, and proportional coefficient. An AMTEC-TEG (thermoelectric generator) combined system was researched in Peng et al. (2019b). They were shown that the maximum efficiency of the hybrid system is reached 34%. Wu et al. (2017) investigated the AMTEC/TEG hybrid system parametrically. They found that the maximum efficiencies are 27.42% and 31.33% for AMTEC and AMTEC/TEG respectively. Wu et al. (2019) proposed a new system as an AMTEC-triple effect absorption refrigeration system to meet heating and cooling needs. They revealed that the maximum exergetic efficiency of the hybrid system is 42.7%,

* Corresponding author.
E-mail addresses: lgchenna@yahoo.com, lingenchen@hotmail.com (L. Chen).

https://doi.org/10.1016/j.egyr.2019.11.108

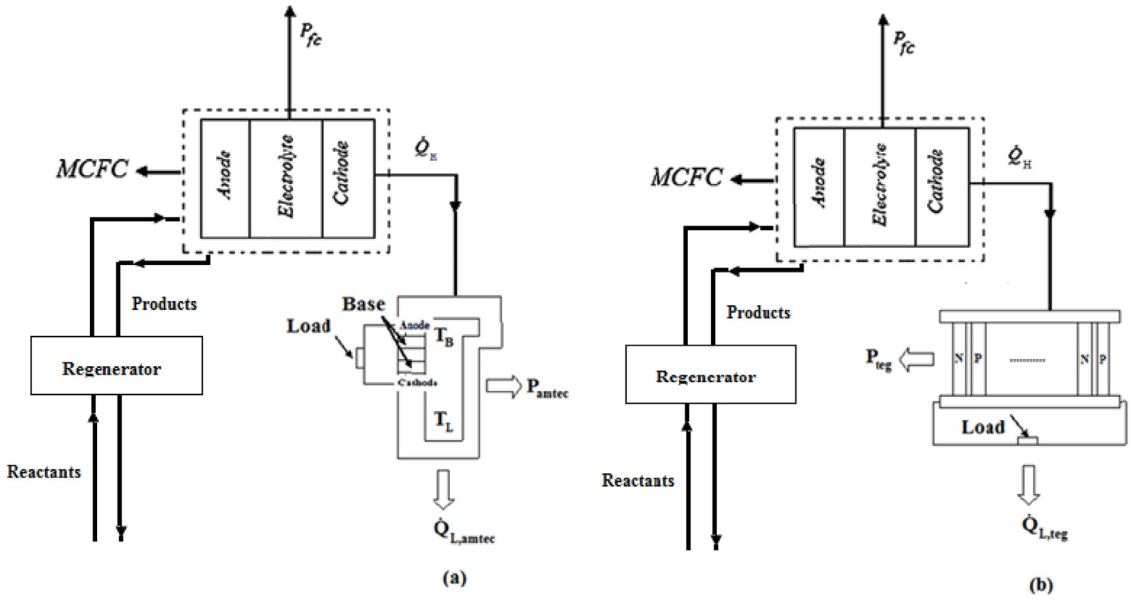

Fig. 1. Schematic of the systems I (a) II (b).

the output power is 48.8 kW and the cooling rate is 110.2 kW. Direct Carbon Fuel Cell - AMTEC was investigated in terms of its performance (Peng et al., 2019a). They found that maximum power density was 810 (W/m^2) and showed advantages of the coupling system.

Similar to AMTEC, TEGs (thermoelectric generators) have several advantages like; not having moving part, no maintenance, and silent. Thermoelectric generators and coolers are composed of P-type and N-type semiconductor elements. Electricity production from a thermoelectric module is based on the Seeback effect. The most important disadvantage of the TEG is the low figure of merit materials, which cause lower energy efficiency. Researches to develop more efficient TEG has been continued for decades, in this way, wasted heat can be utilized much more to generate power. In the open literature, there are some investigations of thermoelectric generators (Arora et al., 2015; Chen et al., 2002; Meng et al., 2011; Guo et al., 2019a,b) and these papers were focused on the maximization of the power output and efficiency. Another criterion is the stage number or serial–parallel configurations for the TEGs. Arora et al. (2015), researched two stages of thermoelectric generator for serial and parallel configurations by means of NSGA-II method. Chen et al. investigated the performance of the TEG in terms of heat transfer influence (Chen et al., 2002). Numerical analysis was researched for TEG with multi-irreversibilities in Meng et al. (2011). They considered finned heat exchangers as heat transfer equipment and found that the maximum power output is 0.13 W and the maximum efficiency is 87%. Polymer Electrolyte Membrane Fuel Cell (PEMFC)-TEG integrated system was taken into account by Guo et al. (2019a). They conducted energy and exergy analysis for the system and the Thomson effect was considered in analyses. Results showed that the performance of the combined system increases by more than 10% comparing the performance of the PEM. High-Temperature PEM fuel cell (HT-PEMFC)-TEG combined system was researched in Guo et al. (2019b). They revealed that the power output of the combined system improves by around 21%.

Aim of this paper is to propose AMTEC as a subsystem for utilizing waste heat of an MCFC and compare the proposed hybrid system with another one, the MCFC-TEG system. The efficiency of the TEG is low, owing to low figure of merit of the material. However, AMTEC has better heat transfer performance because it is filled with a working fluid having better thermal properties. This leads AMTEC to have better performance than TEG. Performance assessment of the AMTEC and its hybrid applications are limited in the literature. In this paper, this shortage is tried to fill. Performance investigation of the AMTEC including exergy based is performed. Performance analyses are conducted according to current density change. Power density, energy efficiency, exergy efficiency, exergy destruction density are taken into account as performance parameters. Numerical calculations are made, results are discussed and the most efficient conditions are described. The performances are compared between two hybrid systems.

2. System description

The MCFC-AMTEC and the MCFC-TEG hybrid system are studied in this paper. The MCFC-AMTEC hybrid system is called hybrid I and the MCFC-TEG the hybrid system is called hybrid II. Schematic of the hybrid I and II are illustrated in Fig. 1.

The hybrid I consists of an MCFC and AMTEC. MCFC is a fuel cell that uses a molten carbonate salt as the electrolyte. Main principle of the MCFC is to generate electricity by means of electrochemical reaction. H_2 is the fuel and air is the oxidant and water, electricity and heat are products. The chemical reaction is described as: $H_2 + 0.5\ O_2 + CO_2 \longrightarrow H_2O + CO_2 +$ heat + electricity. Its characteristic property is to obtain heat at nearly 650 °C, this high operating temperature is utilized to enhance reaction kinetics, thus it is not required to use a noble metal catalyst. Another advantage is that higher temperature makes fuel cell more safety against carbon monoxide poisoning and MCFC systems can be used with different fuels. The disadvantage of MCFC is to use a liquid electrolyte and it is needed to inject carbon dioxide and some problems about high temperature and corrosive properties of the electrodes. The reason for being chosen MCFC as the main energy provider is to be used in large stationary power generation. It can be operated in megawatt capacity and they have really high efficiency.

In this paper, heat removed from the MCFC is only considered to produce electricity and heating or cooling applications are ignored. AMTEC systems convert thermal energy to electricity directly such as TEG. However, their operating principles are quite

different. In the AMTEC, there are some elements called BASE elements and they are connected in series to provide a higher output voltage. BASE elements split AMTEC into two regions. The first of these regions is the high-pressure cavity which is the high-pressure cavity, and the second is the low-pressure cavity. Sodium or potassium can be used as a working fluid. In this study, sodium is chosen as a working fluid.

The operation way of the hybrid system I can be described as follows. Operating heat is provided by the heat released from the MCFC and then enters a high pressure cavity. Sodium ionization happens at the anode, the sodium ions spread to the cathode because of the pressure difference. The electrons circulate and produce power. Finally, ions reach the cathode and they recombine with the sodium ions (Peng et al., 2019b).

Hybrid II is composed of a combination of MCFC and TEG. Heat rejected from the MCFC is send to TEG where additional electricity is produced directly. The TEG is a device which has advantages to recycle the waste heat to generate electrical energy. A thermoelectric module is comprised of p- and n-type semiconductors connected in series or parallel. The electricity generation principle is known as the Seebeck effect.

3. Performance analyses

Schematic of MCFC-heat engine system is shown in Fig. 1a. The waste heat of the MCFC is utilized by the bottom cycle as heat input and extra power output is provided. Firstly, some basic parameters are defined to analyze the performance of MCFC. They are (Zhang et al., 2011):

Anode potential (U_{an}):

$$U_{an} = 2.27 \times 10^{-9}\, je^{\left(\frac{E_{act,an}}{RT}\right)} p_{H_2,an}^{-0.42}\, p_{CO_2,an}^{-0.17}\, p_{H_2O,an}^{-1} \tag{1}$$

Cathode potential (U_{cat}):

$$U_{cat} = 7.505 \times 10^{-10}\, je^{\left(\frac{E_{act,cat}}{RT}\right)} p_{O_2,cat}^{-0.43}\, p_{CO_2,cat}^{-0.09} \tag{2}$$

Ohm overpotential (U_{ohm}):

$$U_{ohm} = 0.5 \times 10^{-4}\, je^{\left(3016\left(\frac{1}{T}-\frac{1}{923}\right)\right)} \tag{3}$$

Theoretical maximum potential (U_o):

$$U_o = E_o + \frac{RT}{n_e F} \ln\left(\frac{p_{H_2,an}\left(p_{O_2,cat}\right)^{0.5} p_{CO_2,cat}}{p_{H_2,an}\, p_{CO_2,an}}\right) \tag{4}$$

where j represents the current density; $p_{H_2,an}$, $p_{CO_2,an}$ and $p_{H_2O,an}$ are partial pressure of the hydrogen, carbon dioxide and water at the anode respectively; $p_{O_2,cat}$ and $p_{CO_2,cat}$ are the partial pressures of oxygen and the carbon dioxide at the cathode; R represents the universal gas constant; T represents the fuel cell temperature, which is utilized by the bottom cycle; the activation energy is E_{act} an E_o is the ideal standard potential which is written as:

$$E_o = 1.2541 - 2.3734 \times 10^{-4} T \tag{5}$$

where F and the n_e represent Faraday constant and the number of electrons respectively.

Cell voltage is described as:

$$U_{fc} = (U_o - U_{an} - U_{cat} - U_{ohm}) \tag{6}$$

Power output from the stack is defined as:

$$P_{fc,stack} = U_{fc}\, jA_{fc} \tag{7}$$

Hydrogen and oxygen is bellowed up by compressors. Power of the compressors of the hydrogen and the air can be seen in Eqs. (8) and (9):

$$P_{hy,c} = \frac{\dot{m}_{hy}\, c_{p,hy}\, T_o}{\eta_{hy}} \left(r^{\frac{\gamma-1}{\gamma}} - 1\right) \tag{8}$$

$$P_{air,c} = \frac{\dot{m}_{air} c_{p,air} T_o}{\eta_{air}} \left(r^{\frac{\gamma-1}{\gamma}} - 1\right) \tag{9}$$

where, c_p is the specific heat, η is the isentropic efficiency of the compressors and they are assumed as 0.6, γ is the adiabatic coefficient. Net power provided by the fuel cell:

$$P_{fc} = P_{fc,stack} - P_{hy,c} - P_{ox,c} \tag{10}$$

Energy efficiency is described as ratio of the obtained energy to energy input. For the MCFC, heat obtained from the fuel cell is utilized for generating electricity at the AMTEC or TEG, besides the power output. Hence, heat is added to equation as useful energy and energy efficiency is described as:

$$\eta_{fc} = \frac{P_{fc} + \dot{Q}_H}{\dot{m}_{H_2}\, LHV_{H_2}} \tag{11}$$

Similar to energy efficiency, fuel cell exergy efficiency can be defined as:

$$\varphi_{fc} = \frac{P_{fc} + \dot{Q}_H\left(1 - \frac{T_o}{T}\right)}{\dot{m}_{H_2}\phi LHV_{H_2}} \tag{12}$$

where, ϕ is an exergetic cofficient. Exergy destruction of the cell is (Zhang et al., 2010):

$$Exd_{fc} = \left(-\frac{\Delta h}{n_e F} - U_{fc}\right) jA_{fc} \tag{13}$$

Regenerator heat is:

$$\dot{Q}_{reg} = K_{reg}(1 - \varepsilon_{reg})(T - T_o) \tag{14}$$

K_{reg} and ε_{reg} are the heat transfer conductance and efficiency of the regenerator. The rejected heat from the fuel cell is expressed in Eq. (15):

$$\dot{Q}_H = -\Delta H - P_{fc} - \dot{Q}_r \tag{15}$$

Heat input to the AMTEC is described as (Peng et al., 2018, 2019b; Wu et al., 2017, 2019):

$$\dot{Q}_{H,amtec} = \frac{NA_{amtec} jM}{F}\left(c_p\left(T_B - T_{cd}\right) + L\left(T_B\right)\right) + NA_{amtec}\, j\frac{RT_B}{F} ln\frac{p_a}{p_c} + \frac{NA_{amtec}\sigma}{Z}\left(T_B^4 - T_{cd}^4\right) \tag{16}$$

Pressure of sodium vapor at the anode (Pa) is (Peng et al., 2018, 2019b; Wu et al., 2017, 2019):

$$p_a = p_{sat}(T_B) p_c \tag{17}$$

Pressure of sodium vapor at the cathode (Pa) is (Peng et al., 2018, 2019b; Wu et al., 2017, 2019):

$$p_c = p_c^{oc} + \Delta p_{cd} \tag{18}$$

where p_c^{oc} is open-circuit sodium vapor pressure at the cathode (Pa), and Δp_{cd} is vapor pressure loss at the cathode (Pa) (Peng et al., 2018, 2019b; Wu et al., 2017, 2019):

$$\Delta p_{cd} = \frac{3G}{8\pi}(2\pi MRT_B)^{0.5}\frac{j}{F} \tag{19}$$

The open-circuit voltage (V) of the AMTEC is (Peng et al., 2018, 2019b; Wu et al., 2017, 2019):

$$U_{oc} = \frac{1}{f} ln\frac{p_{sat}\left(T_B\right)}{p_{sat}\left(T_{cd}\right)\sqrt{T_B T_{cd}}} \tag{20}$$

The over potential difference (V) is (Peng et al., 2018, 2019b; Wu et al., 2017, 2019):

$$U_{ac} = -\frac{2}{f} ln \left[\begin{array}{l} \frac{1}{2}\left[\frac{j^2 T_B}{B^2 p_{sat}^2 (T_{ev})} + 4\right]^{0.5} \\ -\frac{1}{2}\frac{j\sqrt{T_B}}{B p_{sat}(T_B)} \end{array} \right] + \frac{2}{f} ln \left[\begin{array}{l} \frac{1}{2}\left[\frac{j^2\sqrt{T_B T_{cd}}}{B^2 p_{sat}(T_{ev}) p_{sat}(T_{cd})} + 4\left[1 + \frac{\Delta p_{cd}\sqrt{T_{cd}}}{p_{sat}(T_{cd})\sqrt{T_B}}\right]\right]^{0.5} \\ +\frac{1}{2}\frac{j (T_B T_{cd})^{0.25}}{B\sqrt{p_{sat}(T_{ev}) p_{sat}(T_{cd})}} \end{array} \right] \quad (21)$$

where;

$$f = \frac{F}{RT_B} \quad (22)$$

Voltage loss (V) is (Peng et al., 2018, 2019b; Wu et al., 2017, 2019):

$$U_r = j\rho_B D \quad (23)$$

Voltage of the AMTEC is (Peng et al., 2018, 2019b; Wu et al., 2017, 2019):

$$U_{amtec} = U_{oc} - U_{ac} - U_r \quad (24)$$

where ρ_B is ionic resistivity of BASE (Ω m) (Peng et al., 2018, 2019b; Wu et al., 2017, 2019):

$$\rho_B = 1.62 \times 10^{-5} T_B e^{\left(\frac{-45.5}{T_B}\right)} + 1.55 \times 10^{-7} T_B e^{\left(\frac{3772}{T_B}\right)} \quad (25)$$

The vapor pressure of the condenser can be calculated by the following equation (Peng et al., 2018, 2019b; Wu et al., 2017, 2019):

$$\frac{p_{sat}(T_B)}{1 + p_{sat}(T_B)\frac{\lambda D}{RT_B}} = p_{sat}(T_{cd})\sqrt{\frac{T_B}{T_{cd}}} \quad (26)$$

Power obtained from the AMTEC (W) is (Peng et al., 2018, 2019b; Wu et al., 2017, 2019):

$$P_{amtec} = V_{amtec} j A_{amtec} \quad (27)$$

Heat rejected from the AMTEC (W) is

$$\dot{Q}_{L,amtec} = \dot{Q}_H - P_{amtec} \quad (28)$$

Exergy destruction of the AMTEC (W) is

$$Exd_{amtec} = \left(\frac{\dot{Q}_{amtec,L}}{T_L} - \frac{\dot{Q}_H}{T_B}\right) \quad (29)$$

Energy efficiency of the AMTEC is

$$\eta_{amtec} = \frac{P_{amtec}}{\dot{Q}_{amtec,H}} \quad (30)$$

Exergy efficiency of the AMTEC is

$$\varphi_{amtec} = \frac{P_{amtec}}{\dot{Q}_{out,amtec}\left(1 - \frac{T_o}{T_B}\right)} \quad (31)$$

Heat input of thermoelectric generator and heat rejected from the thermoelectric generator are as follows (Chen et al., 2002):

$$\dot{Q}_{H,teg} = N\left(\beta I T - I^2\frac{r}{2} + K(T - T_L)\right) \quad (32)$$

$$\dot{Q}_{L,teg} = N\left(\beta I T_L + I^2\frac{r}{2} + K(T - T_L)\right) \quad (33)$$

where Seebeck coefficient is β, N is the amount of the thermoelectric units, I is the current of the thermoelectric units, the hot junction temperature is T, the cold junction temperature is T_L, electric resistance is the r, and K represents the thermal conductance. Power obtained from thermoelectric generator is (W):

$$P_{teg} = \dot{Q}_{H,} - \dot{Q}_{L,teg} \quad (34)$$

Exergy destruction rate (W/K) is

$$Exd_{teg} = \left(\frac{\dot{Q}_{teg,L}}{T_L} - \frac{\dot{Q}_H}{T}\right) \quad (35)$$

Energy efficiency is

$$\eta_{teg} = \frac{P_{teg}}{\dot{Q}_{teg,H}} \quad (36)$$

Exergy efficiency is

$$\varphi_{teg} = \frac{P_{teg}}{\dot{Q}_{out,teg}\left(1 - \frac{T_o}{T}\right)} \quad (37)$$

Thermoelectric properties depending on temperature are as follows (Xuan et al., 2002):

$$\beta = 2 \times (22224 + 930.6T_m - 0.9905{T_m}^2) \times 10^{-9} \quad (38)$$

$$\rho_p = \rho_n = (5112 + 163.4T_m - 0.6279{T_m}^2) \times 10^{-10} \quad (39)$$

$$\lambda_p = \lambda_n(62605 - 277.7T_m + 0.413{T_m}^2) \times 10^{-4} \quad (40)$$

$$T_m = \left(\frac{T + T_L}{2}\right) \quad (41)$$

$$r = \left(\frac{\rho_p + \rho_n}{C}\right) \quad (42)$$

$$K = \left(\frac{\lambda_p + \lambda_n}{C}\right) \quad (43)$$

where, T_m is the mean temperature and C is the geometry factor.

Therefore, the thermodynamic parameters including power, energy efficiency, exergy efficiency and exergy destruction rate, of hybrid I and II areas followings:

$$P_I = P_{fc} + P_{amtec} \quad (44)$$

$$P_{II} = P_{fc} + P_{teg} \quad (45)$$

$$Exd_I = Exd_{fc} + Exd_{amtec} \quad (46)$$

$$Exd_{II} = Exd_{fc} + Exd_{teg} \quad (47)$$

$$\eta_I = \frac{P_I}{\dot{m}_{H_2} LHV_{H_2}} \quad (48)$$

$$\varphi_I = \frac{P_I}{\dot{m}_{H_2}\phi LHV_{H_2}\Phi} \quad (49)$$

$$\eta_{II} = \frac{P_{II}}{\dot{m}_{H_2} LHV_{H_2}} \quad (50)$$

$$\varphi_{II} = \frac{P_{II}}{\dot{m}_{H_2}\phi LHV_{H_2}\Phi} \quad (51)$$

Table 1
Parameter values used in calculations.

Parameter	Unit	Value
$p_{H_2,an}$, $p_{H_2O,an}$, $p_{CO_2,an}$	atm	0.6, 0.25, 0.15
$p_{O_2,cat}$, $p_{CO_2,cat}$	atm	0.08, 0.08, 0.25
n_e	–	2
$E_{act,an}$	J/mol^2	53,500
$E_{act,cat}$	J/mol^2	77,300
F	C/mol	96,485
R	J/mol K	8.314
Δh	J/mol	−219,644
$T = T_B$	K	923
T_{cd}	K	400
T_o	K	298.15
T_L	K	300
LHV_{H_2}	J/mol	242 000
L	J/mol	89 000
c_p	J/mol K	30
ϕ	–	0.97
σ	W/m^2 K^4	5.67×10^{-8}
Z	–	50
G	–	10
M	mol/g	23
B	A K$^{1/2}$/Pa m^2	90
D	m	5×10^{-4}
C	m	0.5

4. Results and discussions

Performance comparison between MCFC-AMTEC and MCFC-TEG systems are performed. Analyses include power outputs, energy efficiencies, exergy efficiencies and exergy destructions for the considered two systems. In addition, power output and energy efficiency ($P - \eta$) curves are formed. Fixed input parameters are listed in Table 1. In the calculations, same operating conditions are chosen. Real MCFC systems operate under 1400 A/m^2 current density. Because the actual system must reflect the fuel utilization rate, it is difficult to distribute the gas by supplying very low flow rate of fuel. In addition, low power density is also undesirable, so it is common to operate at a current density of 1400 A/m^2 below the maximum power density. Thus, real operating conditions are investigated too and they are compared to maximum values. Maximum error of models used in this paper for the MCFC, AMTEC and TEG are 3%, 2% and 7%, respectively (Brouwer et al., 2006; Wu et al., 2017).

Fig. 2 shows power densities according to current density. All power density curves have maximum which is called optimum points. MCFC reaches its optimum value at j = 3650 (A/m^2). Optimum points for the AMTEC, TEG, hybrid I and hybrid II are obtained at j = 3650 (A/m^2), j = 2400 (A/m^2), j = 3650 (A/m^2), and j = 3300 (A/m^2), respectively. The corresponding power densities are 1755.210 (W/m^2), 670.623 (W/m^2), 261.06 (W/m^2), 2425.833 (W/m^2), and 1964.389 (W/m^2), respectively. It can be seen that those power densities of AMTEC are bigger than those of the TEG, and power densities of the hybrid I are bigger than those of hybrid II. The smallest power density is provided for the TEG. It is seen that except for the TEG, which is obtained at 2400 (A/m^2), the optimum points are close to each other (between 3300–3650 (A/m^2)). For the real conditions, which is current density is 1400 (A/m^2), the power density of the MCFC, AMTEC, TEG, hybrid I and hybrid II are equal to 1091.250 (W/m^2), 469.950 (W/m^2), 215.802 (W/m^2), 1561.200 (W/m^2), and 1307.052 (W/m^2), respectively. These values are 62%, 70%, 83%, 64% and 66% of their maximum. These values show that there are dramatic decreasing comparing with maximum values for the hybrid systems, however, these are still bigger than 1 kW per square meter.

Fig. 3 reveals the change of energy efficiencies according to current density. AMTEC and TEG have the extremum, while MCFC and the hybrid I and hybrid II do not have. The maximum points

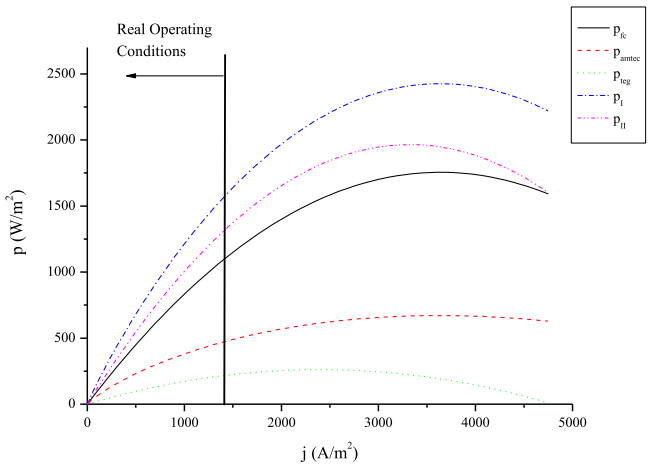

Fig. 2. Variation of the power density with current density.

are obtained at $j = 1100$ (A/m^2) for the AMTEC, and $j = 2300$ (A/m^2) for the TEG. The corresponding energy efficiencies are 16.4% and 2.4% respectively. Energy efficiencies of the MCFC increases and hybrid I and hybrid II decrease with current density and maximum energy efficiencies are 89.8%, 76.6% and 76.4%, respectively. Energy efficiencies of the AMTEC are bigger than those of the TEG and, obviously, energy efficiencies of the hybrid I are bigger than those of hybrid II. TEG has the smallest energy efficiency values comparing to others. As it is explained in the introduction section, TEG has a low figure of merit causing it to reduce energy efficiency. This means that TEG has lower efficiency from the AMTEC and if the same heat input is provided for these two systems, higher power density can be obtained from the AMTEC. For the real operating conditions, efficiencies of the MCFC, AMTEC, TEG, hybrid I and hybrid II are equal to 89.5%, 16.2%, 2.1%, 66.8%, and 62.7% respectively. These results indicate that efficiencies of the MCFC, AMTEC and TEG are nearly the same with their maximum, while energy efficiencies of the hybrid I and II are lower nearly 10%–14%, which are still bigger than 60%. So more than 60% of the input energy can be converted to useful power.

Fig. 4 shows changes of the exergy efficiencies. For exergy efficiencies, results are similar to those for energy efficiencies. AMTEC and TEG have extremum points are the similar with the tendency for energy efficiency. The corresponding exergy efficiencies are 24.2% and 3.6%, respectively. Exergy efficiencies of the hybrid I are bigger than those of hybrid II. Maximum points of the hybrid I, hybrid II and MCFC are equal to 78.1%, 78% and 86.1%, respectively, which decrease with current density. At the operating conditions, MCFC, AMTEC, TEG, hybrid I and hybrid II are 83.17%, 23.9%, 3.1%, 67.9% and 64%, respectively. Exergy efficiencies for the MCFC, AMTEC and TEG are nearly same with their maximum values, other values are 10%–14% lower than their maximums. Exergy efficiency describes how close a system to ideal one and at the operation conditions it still close more than 60% to ideal cycle. This is very promising when comparing other conventional energy conversion devices.

Exergy destruction rate densities are shown in Fig. 5. As can be seen, exergy destruction rate increases dramatically with current density. Results reveal that the exergy destruction rate density of the hybrid II is much greater than that of hybrid I. Similarly, exergy destruction rate density of the TEG is bigger than that of AMTEC and exergy destruction rate density of the MCFC is the smallest one. For the heat engines, exergy destruction can be written as $Exd = \frac{T_o \dot{Q}_H}{T_L}\left(1 - \eta - \frac{T_L}{T_H}\right)$ too. According to this

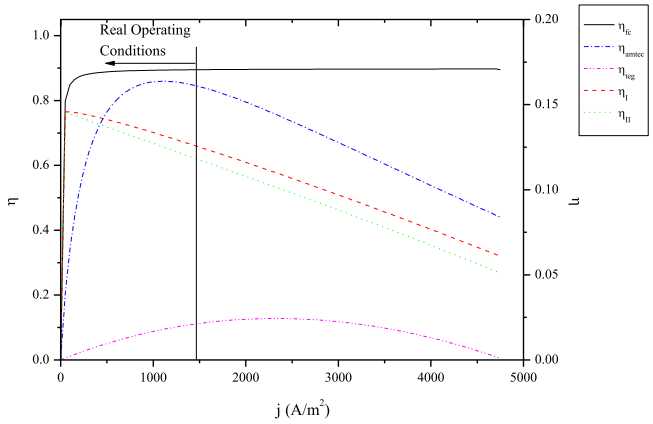

Fig. 3. Variation of energy efficiency with current density.

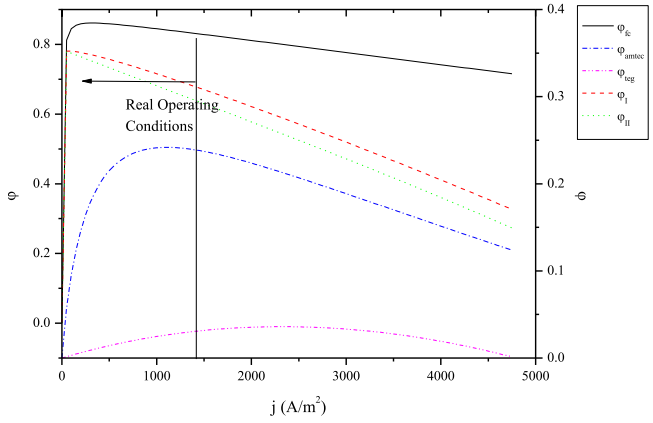

Fig. 4. Variation of the exergy efficiency with current density.

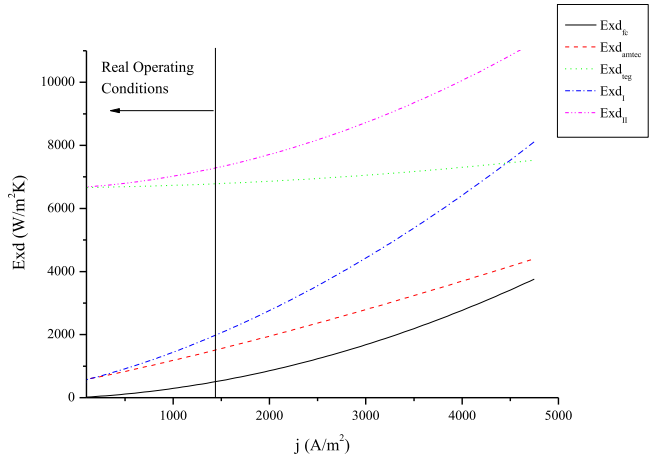

Fig. 5. Variation of the exergy destruction density with current density.

equation, it is obvious that if energy efficiency is lower, exergy destruction is higher providing that T_H and T_L are the same. Therefore, exergy destruction of the TEG is bigger than that of the AMTEC and exergy destruction of the system II is bigger than the hybrid I. For the MCFC, it is not a heat engine, it is an electrochemical device and according to Eq. (13), it is only affected by the electrochemical parameters and as it is a well-known effect of the heat transfer has the most important reason for the entropy generation so exergy destruction. When the results compare to exergy destruction values at the operating conditions,

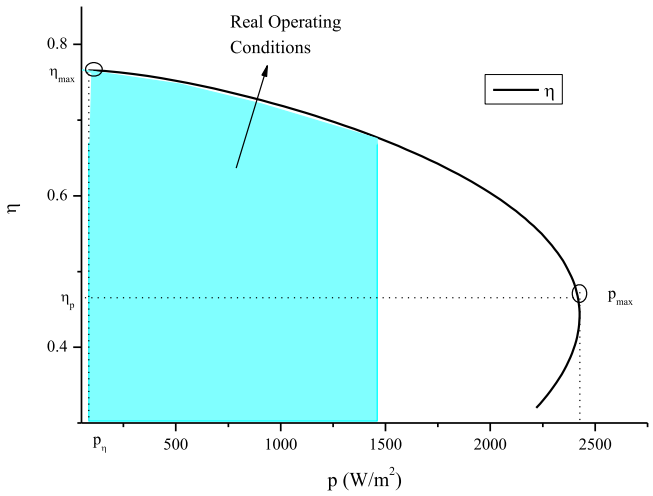

Fig. 6. P-η curve of the system I.

it is obvious that exergy destruction rate density for the hybrid I is nearly lower three times compare the value at the maximum power, similarly it is 20% lower than the value at the maximum power density for the hybrid II.

P-η curves for the hybrid I and II are shown in Figs. 6 and 7. In these curves, P_{max} is the maximum power density, P_η is the power density at the maximum energy efficiency, η_{max} is the maximum energy efficiency and η_p is the energy efficiency at the maximum power density. In addition, the real operating conditions are illustrated in these curves. For the hybrid I, $P_{max} = 2425.833$ (W/m^2) and $P_\eta = 82.810$ (W/m^2), which is only 3.4% of the maximum power; $\eta_{max} = 76.6\%$ and $\eta_p = 44.4\%$, which is 32.2% lower than the maximum efficiency. Similar investigations can be performed for the exergy destruction rate densities. The exergy destruction density rate at the optimum power (Exd_p) is 5684.08 (W/m^2 K) and the exergy destruction density rate at the optimum efficiency (Exd_η) is 8.412 (W/m^2 K) which can be ignored. For hybrid II, $P_{max} = 1964.989$ (W/m^2) and $P_\eta = 58.701$(W/m^2), which is only 3.04% of the maximum power, $\eta_{max} = 76.4\%$ and $\eta_p = 43\%$ which is 33.4% lower than the maximum energy efficiency. Exergy destruction density rate (Exd_p) at the optimum power is 9088.57 (W/m^2 K) and exergy destruction density rate (Exd_η) at the optimum energy efficiency is 6668.822 (W/m^2 K). Exd_η is equal to 73.3% of Exd_p. Lastly, operating conditions are considered, one can see that power density is 64% of its maximum for the hybrid I and 66% for the hybrid II. Similarly, energy efficiency is equal to 67% and 63% for the hybrid I and hybrid II respectively.

According to numerical results, the hybrid I is more advantageous than the hybrid II. Because the power output density, energy efficiency, and exergy efficiency are bigger than those of hybrid II. In addition, the hybrid I is more advantageous than hybrid II in terms of exergy destruction rate density.

The current density for the hybrid systems should be chosen as $j_\eta \leq j \leq j_p$, where j_η and j_p are current densities at the maximum energy efficiency and maximum power. In practice, i.e. operation conditions, efficiency, and power values is high enough as it is expressed above.

The results obtained herein are compared with those obtained in Peng et al. (2018, 2019b,a) for the AMTEC. In this research, the maximum energy efficiency of the AMTEC reaches to 16.4%, while in Peng et al. (2018) the maximum energy efficiency is 22%. However, heat source temperature in that reference is 1170 K and in our study, 923 K. Hence, it is natural that energy efficiency in Peng et al. (2018) is bigger. It can be seen that the power density of AMTEC in this research is nearly three times greater than

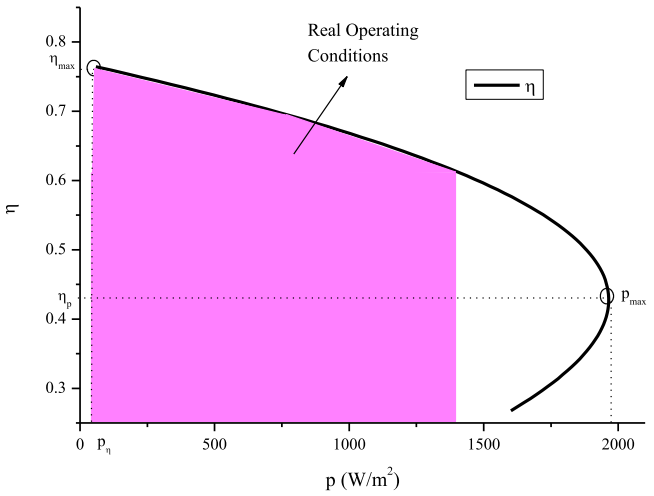

Fig. 7. P-η curve of the system II.

the AMTEC in Peng et al. (2018). However, the thicknesses of the BASE of them are different. In Peng et al. (2019b), the maximum efficiencies of the AMTEC were calculated as 30.9% and 34.1%, they are higher than the maximum efficiency defined herein. Because similar to Peng et al. (2018), heat source temperature in Peng et al. (2019b) (1300 K) is higher than the heat source temperature in this research. Power densities were obtained 60 300 W/m^2 and 46 900 W/m^2, they are higher than the power density in this research. This diversity is resulted from different BASE thickness. As it can be shown in Peng et al. (2019a), the maximum power density of the combined systems is 810 (W/m^2) and for our system it is 2425.833 (W/m^2). Energy efficiency in Peng et al. (2019a) 60% can be achieved. In our system, energy efficiency can reach to 76.6%. One can say that the MCFC-AMTEC system has a higher performance than the DCFC-AMTEC application.

5. Conclusions

This paper compares thermodynamic performances of the MCFC-AMTEC and MCFC-TEG system systems based on the first and second laws of thermodynamics. Performance analyses are carried out in terms of power density, energy efficiency, exergy efficiency, and exergy destruction rate density. Some important results are listed as follows:

(1) The maximum power output densities for the hybrid I and II are 2425.833 (W/m^2) and 1964.389 (W/m^2), respectively.

(2) Energy efficiencies are 76.6% for the system I and 76.4% for the hybrid II.

(3) The hybrid I is more advantageous than hybrid II, current density should be $j_\eta \leq j \leq j_p$,

(4) Using AMTEC is more reasonable than using TEG to be utilized waste heat from the MCFC. It is recommended that deeper analyses including economic and environmental approaches will be needed.

Declaration of competing interest

The authors declare that they have no known competing financial interests or personal relationships that could have appeared to influence the work reported in this paper.

CRediT authorship contribution statement

Emin Açıkkalp: Conceptualization, Data curation, Methodology, Software, Writing — original draft. **Lingen Chen:** Funding acquisition, Supervision, Writing — review & editing. **Mohammad Hosein Ahmadi:** Software, Validation.

Acknowledgments

This paper is supported by The National Natural Science Foundation of China (Grant No. 51576207). The authors wish to thank the reviewers for their careful, unbiased and constructive suggestions, which led to this revised manuscript.

References

Açıkkalp, E., 2017a. Ecologic and sustainable objective performance analysis of molten carbonate fuel cell - Heat engine hybrid system. J. Energy Eng. 143, 04017062.

Açıkkalp, E., 2017b. Ecologic and sustainable objective thermodynamic evaluation of molten carbonate fuel cell - Supercritical CO_2Braytoncycle hybrid system. Int. J. Hydrogen Energy 42, 6272–6280.

Açıkkalp, E., 2017c. Performance analysis of irreversible molten carbonate fuel cell - Braysson heat engine with ecological objective approach. Energy Convers. Manage. 132, 432–437.

Ahmadi, M.H., Jokar, M.A., Ming, T.Z., Feidt, M., Pourfayaz, F., Astaraei, F.R., 2018a. Multi-objective performance optimization of irreversible molten carbonate fuel cell-Braysson heat engine and thermodynamic analysis with ecological objective approach. Energy 144, 707–722.

Ahmadi, M.H., Sameti, M., Pourkiaei, S.M., Ming, T.Z., Pourfayaz, F., Chamkha, A.J., Oztop, H.F., Jokar, M.A., 2018b. Multi-objective performance optimization of irreversible molten carbonate fuel cell–Stirling heat engine–reverse osmosis and thermodynamic assessment with ecological objective approach. Energy Sci. Eng. 6, 783–796.

Arora, R., Kaushik, S.C., Arora, R., 2015. Multi-objective and multi-parameter optimization of two-stage thermoelectric generator in electrically series and parallel configurations through NSGA-II. Energy 30, 242–254.

Brouwer, J., Jabbari, F., Leal, E.M., Orr, T., 2006. Analysis of a molten carbonate fuel cell: Numerical modeling and experimental validation. J. Power Sources 158, 213–224.

Chen, L.G., Gong, J.Z., Sun, F.R., Wu, C., 2002. Effect of heat transfer on the performance of thermoelectric generators. Int. J. Therm. Sci. 41 (1), 95–99.

Guo, X., Zhang, H., Yuan, J., Wang, J., Zhao, J., Wang, F., Miao, H., Hou, S., 2019a. Energetic and exergetic analyses of a combined system consisting of a high-temperature polymer electrolyte membrane fuel cell and a thermoelectric generator with Thomson effect. Int. J. Hydrogen Energy 44, 16918–16932.

Guo, X., Zhang, H., Yuan, J., Wang, J., Zhao, J., Wang, F., Miao, H., Hou, S., 2019b. Performance assessment of a combined system consisting of a high temperature polymer electrolyte membrane fuel cell and a thermoelectric generator. Energy 179, 762–770.

Lee, J.S., Lee, W.H., Chi, R.G., Chung, W.S., Lee, K.B., Rhi, S.H., et al., 2017. Thermal behavior of heat pipe- assisted alkali-metal thermoelectric converters. Heat Mass Transf. 53, 3373–3382.

Meng, F.K., Chen, L.G., Sun, F.R., 2011. A numerical model and comparative investigation of a thermoelectric generator with multi-irreversibilities. Energy 36 (5), 3513–3522.

Peng, W.L., Cai, L., Lin, J., Zhao, Y.R., JChen, J.C., 2019a. The optimal operation states and parametric choice strategies of a DCFC-AMTECcoupling system with high efficiency. Energy Convers. Manage. 195, 360–366.

Peng, W., Li, W., Ye, Z., Su, G., Chen, J., 2019b. Parametric design strategies of an updated alkali metal thermoelectric converter-thermoelectric generator system operating at optimum states. Energy Convers. Manage. 182, 53–59.

Peng, W., Zhang, X., Ye, Z., Chen, J., 2018. Optimum operation states and parametric selection criteria of an updated alkali metal thermal electric converter. Energy Convers. Manage. 168, 230–236.

Weber, N.A., 1974. Thermoelectric device based on Beta-Alumina solid electrolyte. Energy Convers. 14, 1–8.

Wu, S.Y., Guo, G., Xiao, L., Chen, Z.L., 2019. A new AMTEC/TAR hybrid system for power and cooling cogeneration. Energy Convers. Manage. 180, 206–217.

Wu, S.Y., Zhang, Y.C., Yang, H., Xia, L., 2017. Performance evaluation and parametric analysis of AMTEC/TEG hybrid system. Energy Convers. Manage. 154, 118–126.

Xiao, L., Wu, H.Y., Wu, S.Y., Chua, Q.W., 2017. Parametric analysis of condensation heat transfer characteristics of AMTEC wick condenser. Energy Procedia 105, 4698–4705.

Xuan, X.C., Ng, K.C., Yap, C., Chua, H.T., 2002. The maximum temperature difference and polar characteristic of two-stage thermoelectric coolers. Cryogenics 42, 273–278.

Zhang, X., Guo, J., Chen, J., 2010. The parametric optimum analysis of a proton exchange membrane (PEM) fuel cell and its load matching. Energy 35, 5294–5299.

Zhang, H., Lin, G., Chen, J., 2011. Performance analysis and multi-objective optimization of a new molten carbonate fuel cell system. Int. J. Hydrogen Energy 36, 4015–4021.